IOPscience iopscience.iop.org

Home Search Collections Journals About Contact us My IOPscience

Fully-integrated piezoelectric generators from flexible materials

This content has been downloaded from IOPscience. Please scroll down to see the full text.

2014 Smart Mater. Struct. 23 085006

(http://iopscience.iop.org/0964-1726/23/8/085006)

View the table of contents for this issue, or go to the journal homepage for more

Download details:

IP Address: 138.37.211.113
This content was downloaded on 11/10/2014 at 02:41

Please note that terms and conditions apply.

IOP Publishing Smart Materials and Structures
Smart Mater. Struct. 23 (2014) 085006 (7pp) doi:10.1088/0964-1726/23/8/085006

Fully-integrated piezoelectric generators from flexible materials

Alan Colli[1], Richard White[1], Samiul Haque[1] and Pritesh Hiralal[2]

[1] Nokia Research Center, 21 JJ Thomson Avenue, Cambridge CB3 0FA, UK
[2] Centre for Advanced Photonics and Electronics, 9 JJ Thomson Avenue, Cambridge CB3 0FA, UK

E-mail: alan.colli@nokia.com

Received 14 January 2014, revised 15 May 2014
Accepted for publication 21 May 2014
Published 18 June 2014

Abstract

This paper presents a flexible, integrated piezoelectric system that is simultaneously designed to operate as a self-powered touch sensor and as a charge pump and storage device for the long-term accumulation of energy over several pressure cycles. Rectification is achieved by stacking a piezoresistive polymer on top of a piezoelectric polymer, so that the conductivity of the former switches in phase with the generation of charge in the latter, upon application and release of stress. A thin flexible electrochemical capacitor is then stacked onto the structure to store the generated charge. The resulting integrated generator proves a robust device of general applicability, featuring a flexible and deformable nature, a large dynamic range, and simple manufacturing.

S Online supplementary data available from stacks.iop.org/SMS/23/085006/mmedia

Keywords: piezoelectric, piezoresistive, energy-harvesting, sensor, supercapacitor

(Some figures may appear in colour only in the online journal)

Introduction

Energy management is a primary concern in modern mobile devices [1]. As a consequence, there is a continuous drive to improve or replace those technologies that underpin the most power-hungry features, such as touchscreens. On the other hand, the emergence of a new class of low-power autonomous devices, like those used in wearable electronics and wireless sensor networks, is calling for solutions where energy is captured and stored from external sources (e.g., solar power or kinetic energy), rather than provided by a traditional battery [2]. A self-powered sensor, in particular, is a device that can function and communicate remotely by using the power from the very same stimulus it is supposed to transduce.

For kinetic energy harvesting, a lot of interest has been directed towards piezoelectric materials [3]. The piezoelectric effect converts mechanical strain into an electric current or voltage. This strain can come from many different sources, such as human motion, machine motion, low-frequency vibrations, etc. Particularly popular nowadays is the concept of harvesting kinetic energy from the human body. For example, piezo-generators are being currently embedded in walkways or shoes to recover the energy of footsteps [3]. Researchers at Samsung also believe that piezoelectric technologies hold the key to future self-powered touch sensors and wearable artificial skins [4, 5]. It is important to understand, however, that a basic piezoelectric element (intended as a layer of piezoelectric material sandwiched between two metal electrodes) is not yet a suitable DC generator. Indeed, the electrical output of a piezo-element must be rectified in order to pump charge consistently, and extensive research has been devoted to the optimization of the rectifying circuitry, ranging from simple diodes to more complex architectures [6, 7].

A few recent studies have begun to emphasize the benefits of integrating a rectifying mechanism directly into the piezo-element architecture [4, 8–10], rather than relying on external components. Reference [9], in particular, presented a fully-packaged Li-ion battery with an embedded piezoelectric polymer, and showed that the field produced by such polymer upon stress can be exploited to internally charge the DC battery over time. To power remote and wireless sensors, however, a (super)capacitor would represent a much simpler and environmentally-friendly reservoir to store any harvested

 © 2014 IOP Publishing Ltd Printed in the UK

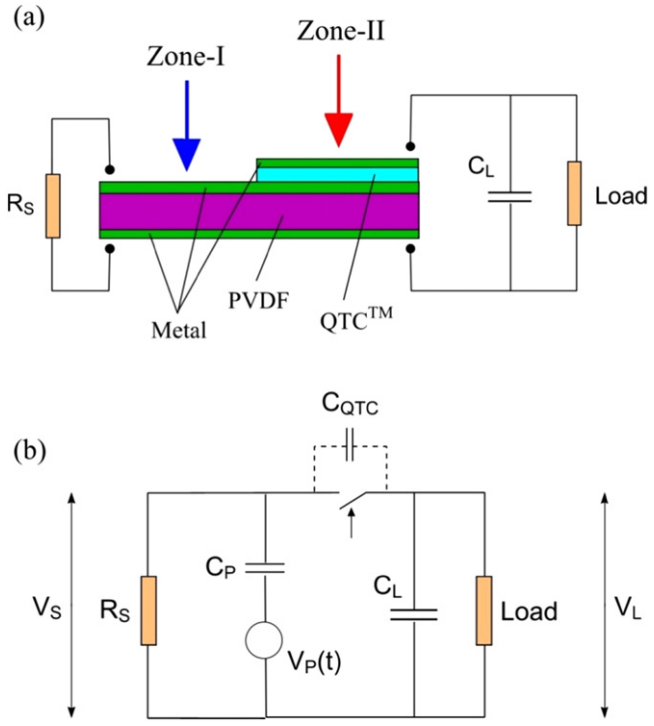

Figure 1. (a) Schematics and (b) equivalent circuit of the tailored structure used to evaluate the behavior of our integrated piezoelectric device.

energy, as the latter would be typically released in single bursts to perform periodic read-out and communication functions. Moreover, for systems that harvest energy from the application of stress and pressure, one has to consider the potential for scaling up a single integrated generator to form a large array of independent pixels, from the relatively small size of a touchscreen pixel to the fairly large area of a floor tile.

Here we present an integrated piezoelectric system that is simultaneously designed to operate as a self-powered touch sensor and as a charge pump and storage device for the long-term accumulation of energy over several pressure cycles. We achieve rectification by stacking a piezoresistive polymer on top of a piezoelectric polymer, so that the conductivity of the former switches in phase with the generation of charge in the latter, upon application and release of stress. A thin flexible capacitor is then added to the structure to store the spikes of generated charge, and release it to a load in a smooth and continuous fashion. The resulting integrated generator proves a robust device of general applicability, featuring a flexible and deformable nature, a large dynamic range, and simple manufacturing. We also show it is ideally scalable to realize functional pixelated structures on any scale and for various applications.

Experimental methods

To fully understand and characterize the behavior of our piezoelectric system, we fabricated the tailored structure schematically illustrated in figure 1(a). Here, a quantum-tunneling-composite (QTC™) piezoresistive film [11–13] sandwiched between metallic contacts is glued on top of a PVDF film also with electrodes on both sides. The piezoelectric element used for this work was obtained from Measurement Specialties (part number: LDT1-028K). It consists of a thin PVDF film (1 cm × 3 cm in size) with Ag electrodes and laminated to a sheet of polyester (Mylar). The piezoresistive material is a 10 μm-thick screen-printable QTC™ film, a proprietary technology from Peratech [11]. The QTC™ film is sandwiched between two planar carbon ink electrodes, forming an element of area $\sim$1 cm^2. With no stress applied, the element is virtually an insulator. Upon pressures of 1–10 N, the element resistance falls in the 1–10 K Ω range. The piezoelectric and piezoresistive elements are stacked together so they could share a common electrode (figure 1(a)). The QTC™ element covers only one half of the total area of the PVDF element, in order to allow the selective application of pressure either on the PVDF element alone (zone-I) or on the PVDF + QTC™ stack (zone-II). External electrical components are then wired to different metal electrodes (figure 1(a)) to easily study the optimal parameters for the generator circuit (these components will eventually be integrated into the flexible structure). R_S values between 1–1000 M Ω (larger than the QTC™ resistance under pressure) were tested with equivalent results (see supporting information). For all experiments reported here $R_S = 100$ M Ω. The output voltages V_L and V_S were measured by means of a LeCroy LC334AM oscilloscope.

The flexible electrochemical capacitor was prepared following a method inspired by [14, 15]. The electrodes were made from a mixture of 95% activated carbon (Norit) and 5% binder (carboxymethylcellulose and PTFE) in water. The mixture was homogenized into a paste and bar coated onto 25 μm-thick carbon coated aluminum foils (Intelicoat technologies). A 60 μm cellulose separator was placed between two electrodes and wetted with a 3M KCl solution as the electrolyte. The sandwiched assembly was laminated in polypropylene sheets, with protruding aluminum contacts for external connection.

The electrical simulations were computed using LTspice v4.15b, available from Linear Technology Corporation. The mechanical durability test was performed using a bending system Lloyd LRX with a 50 N load cell. The sample was first attached with a double sided tape onto a solid base to prioritize compression over bending. The test was then allowed to run for 50 000 cycles with an average force of 10 N per cycle.

Results

The equivalent circuit of the device under test is shown in figure 1(b), and it closely resembles one of the simplest charge-pumping circuits to harvest energy from a piezoelectric element (see for example figure 6(a) in [7]), which is modeled here as a time-dependent voltage generator (V_P) in series with a capacitor (C_P is the intrinsic capacitance of the PVDF element). The key difference is that the diode used for

rectification is replaced by a pressure-controlled switch. Essentially, when pressure is applied on zone-II, the QTC™ film resistance drops well below R_S, and the charge induced by the piezo-element is preferentially stored into the load capacitor C_L. When the pressure is released though, the QTC™ film becomes an insulator, breaking the electrical connection between C_P and C_L. Hence, the capacitor C_P has no other choice than to discharge through R_S before another cycle could begin. As a net result, a DC voltage V_L develops across the load.

An important condition must be fulfilled to validate this idea. In figure 1(b), we emphasize that a QTC™ film sandwiched between two planar electrodes has an intrinsic capacitance C_{QTC}. For efficient charge pumping, C_{QTC} needs to be much smaller than C_P. This is indeed the case for our device, since the measured values for C_P and C_{QTC} are 1.4 nF and 15 pF, respectively.

According to the values chosen for the load and C_L, different operational modes can be achieved. For example, if the device is supposed to work as a self-powered sensor to detect individual touch events, it is desirable to produce an output with the maximum voltage-per-pulse (i.e., reducing C_L to be on the same order of C_P), and to fully discharge C_L before another event can occur (i.e., using a relatively small load). Conversely, if one wants to slowly build up V_L accumulating charge (and energy) into a $C_L \gg C_P$ over several pressure cycles, then a relatively large load should be used to prevent the continuous and competing discharge of C_L.

In figure 2 we investigate the first operational regime by applying 5 N pressure pulses at a frequency of about 1 Hz. We choose $R_S = 100\,\mathrm{M}\Omega$, $C_L = 10$ nF and a load of $1\,\mathrm{M}\Omega$. For a single pulse, the application and the release of pressure are separated by ~200 ms. This is a realistic approximation of the action of tapping a finger. The simultaneous evolutions of V_L and V_S are plotted in figure 2(a) for two pressure pulses applied to zone-I and zone-II. For zone-I pulses, since the QTC™ is in an insulating state at all times, V_L is not affected by the action. The measured V_S closely reflects the typical response of a piezo-element shorted through a resistor: a voltage peak (negative for this particular device) develops upon the application of pressure until C_P is charged, then, as the pressure is removed, the discharge of C_P leads to a complementary peak of positive voltage. If a pressure pulse is applied to zone-II, however, the QTC™ film turns temporarily conductive, and the right branch of the circuit in figure 1 is allowed to participate in the charging. Hence, a negative V_L peak develops in response to the application of pressure. Crucially, there is no positive V_L peak as the pressure is lifted, because the QTC™ reverts to its insulating state and the discharging occurs entirely through R_S, similarly to zone-I events. This proves that the QTC™ is fast enough as a pressure switch for effective rectification of the piezoelectric signal. Note that the peak negative value measured for V_S in zone-I is roughly 7× larger than the peak value for V_L in zone-II. This V_S/V_L peak ratio follows the capacitance ratio C_L/C_P.

The reliability and reproducibility of all the above features are visible in figure 2(b), where both V_L and V_S are

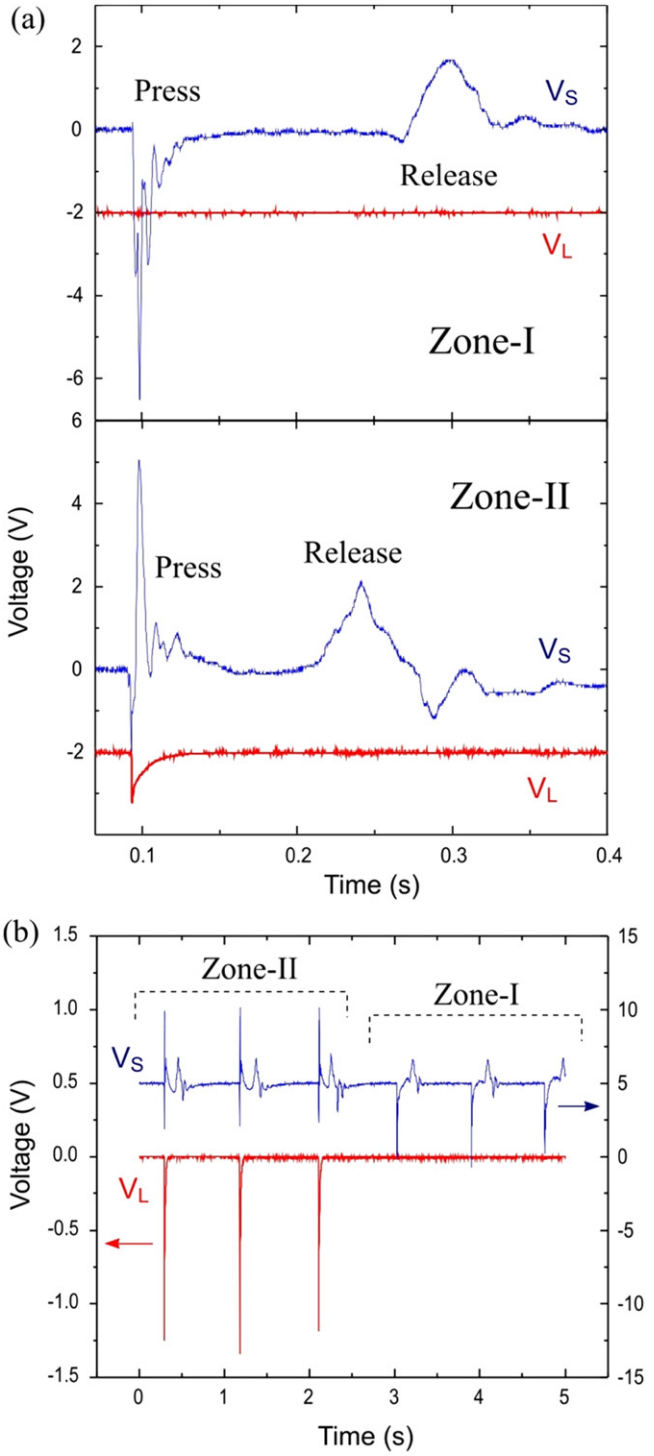

Figure 2. (a) Different evolution of V_S and V_L over a single pressure cycle (press + release) as stress is applied to zone-I or zone-II. V_L is shifted by −2 V for clarity. (b) Evolution of V_S and V_L over multiple pressure cycles on different zones, showing the consistency of the system response. V_S is shifted by 5 V for clarity.

plotted over a series of six consecutive pressure pulses, the first three applied on zone-II, the remaining ones on zone-I. Accordingly, if used as a touch sensor, this device would produce a prompt, smooth, and consistent DC output for any 'press' event on the active area (zone-II), irrespective of the

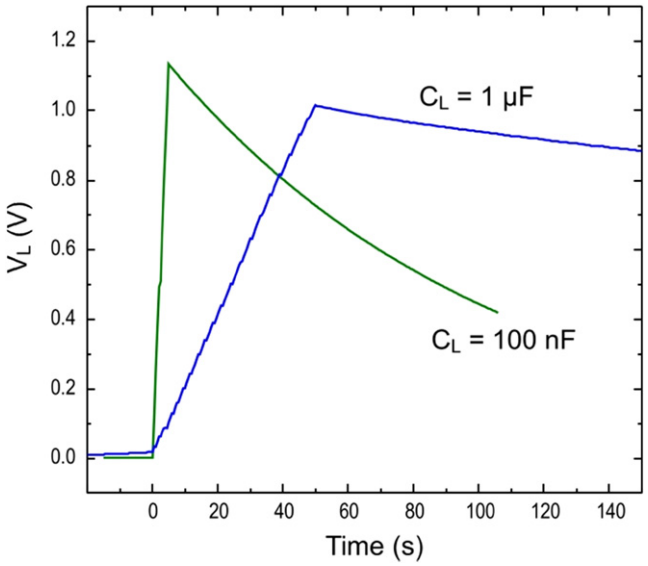

Figure 3. Charge accumulation regime for our piezoelectric generator. Higher values for C_L allow more energy storage, but more pressure cycles are needed to achieve the same V_L.

overall (and arbitrary) duration of individual touch events (i.e., how long the finger is kept down before release).

In figure 3 we use bigger values for C_L and a load of 1 G Ω to investigate the energy-harvesting and charge accumulation regime of our integrated piezo-generator. We apply 5 N pressure pulses on zone-II at a rate of about 2 Hz until a V_L of roughly 1 V is reached. Then, we let the system slowly discharge according to its specific time constant (1 G Ω* C_L). Unsurprisingly, the number of pulses needed to generate $V_L = 1$ V (m) scales linearly with C_L. For $C_L = 10$ nF (figure 2), a single pulse was sufficient. Increasing C_L to 100 nF and 1 μF requires roughly 10 and 100 pulses, respectively (i.e., 5 and 50 s in figure 3). This allows us to easily calculate the average charge per pulse that is pumped into C_L, which turns out to be (1 V* C_L)/m = 10^{-8} C.

Following the fundamental characterization above, we have assembled a fully-packaged piezoelectric DC generator by integrating both the R_S resistor and the load capacitor C_L into a single flexible structure. Figure 4(a) schematically illustrates how the components are stacked and connected, while a picture of the physical prototype is shown in figure 4(b). We have used a narrow piece of carbon tape to connect together the PVDF electrodes ($R_S \sim 40$ M Ω), and conductive copper tape for the metallic connections between different components. The load capacitor on the back of the structure is a flexible supercapacitor ($C_L \sim 1$ mF) fabricated *ad-hoc* (see experimental methods). It is obvious from figure 3 that this prototype requires a very large number of pressure cycles (and a nominally infinite load under charging) to build up a significant V_L. Since our supercapacitor also showed a small leakage under bias, we could not achieve saturation values for V_L larger than a few mV. It is thus important that the capacitor or supercapacitor, when needed, is carefully chosen to match the amount of charge supplied by the piezoelectric pump in a defined regime of operation.

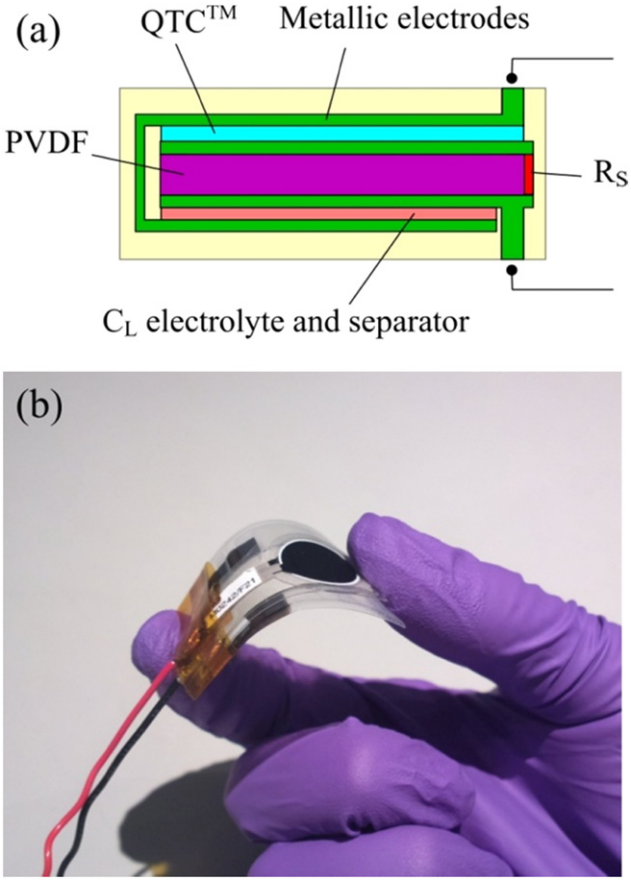

Figure 4. (a) Schematics and (b) photograph of a fully-integrated piezoelectric generator made entirely from flexible materials.

Discussion

We estimated above that the average charge that can be pumped per unit area in response of a fixed amount of pressure is about 2 nC N^{-1} cm^{-2}. This is an acceptable value but, although it could be further improved by optimizing specifications like the PVDF and the QTC™ thickness, it is unlikely to match the most efficient piezoelectric generators to date, where crystals with higher piezoelectric coefficients are used and rectification is achieved by more sophisticated circuit architectures [6, 7]. It is thus crucial to understand that the most important and unique benefits of our integrated piezo-generator device are essentially twofold: first, it is very robust and durable but at the same time very straightforward to fabricate; second, by providing a built-in solution for local rectification, it potentially allows the realization of very large area devices with an efficient response to local stimuli, i.e., devices that work well when the pressure is applied only on a small fraction of the total area. We thus steer the following discussion towards the evidence supporting these specific claims.

Both the PVDF and the QTC™ components, taken individually, have specifications as commercial products (see Experimental Methods). PVDF is also extensively studied in applied research, and its durability to stress cycles is measured in the millions [16]. The QTC™ film as provided by

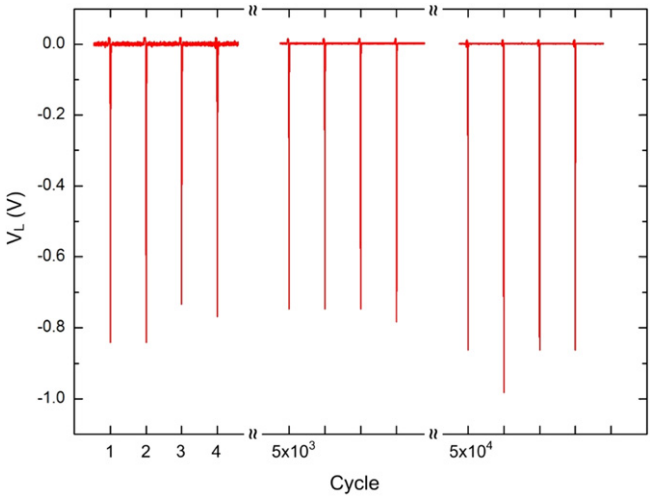

Figure 5. Output voltage V_L measured for 50 000 press/release cycles, showing no degradation of device performance.

Peratech claims a lifetime of one million cycles for forces up to 50 Kg. Nevertheless, we have performed a simple 50 000 cycles stress test for an integrated device similar to that studied in figure 2, more with the purpose of evaluating the robustness of the overall package than to confirm the durability of its building blocks. The results reported in figure 5 show that there is no visible degradation of the output signal V_L after 50 000 cycles. This shows that our device concept is not just based on durable materials, but also that long-term robustness can be achieved by a cheap and straightforward assembly strategy. This is crucial for some large area manufacturing techniques like, e.g., roll-to-roll fabrication.

The second major benefit of our integrated piezo-generator is inherent to its internal design. When assessing generators based on arbitrary piezoelectric elements and associated rectification circuitry, it is often assumed that the applied stress is distributed uniformly across the entire active area. In many practical energy-harvesting applications, however, the stimulated area is only a fraction of the total surface (e.g., a finger touch on a screen or a footstep on a carpet). If a very localized stress is applied on a large piezoelectric element, one can model the structure as an array of $n+1$ capacitors in parallel (each having an area equal to the stimulated area), of which only one (0) is driven by the polarization of the piezoelectric material (figure 6(a)). The n inactive capacitors present a detrimental parasitic capacitance to the signal generated at stage (0). Ideally, the total area of the generator should be divided into autonomous pixels (or tiles) roughly matching the lateral size of the stimulus, each of them with their own rectifying circuitry (figure 6(b)). To quantify this argument, we perform a simple simulation and compare the circuit geometries in figures 6(a) and (b) for a V_P drive made of 200 pulses[3]. We then plot in figure 6(c) the final open-

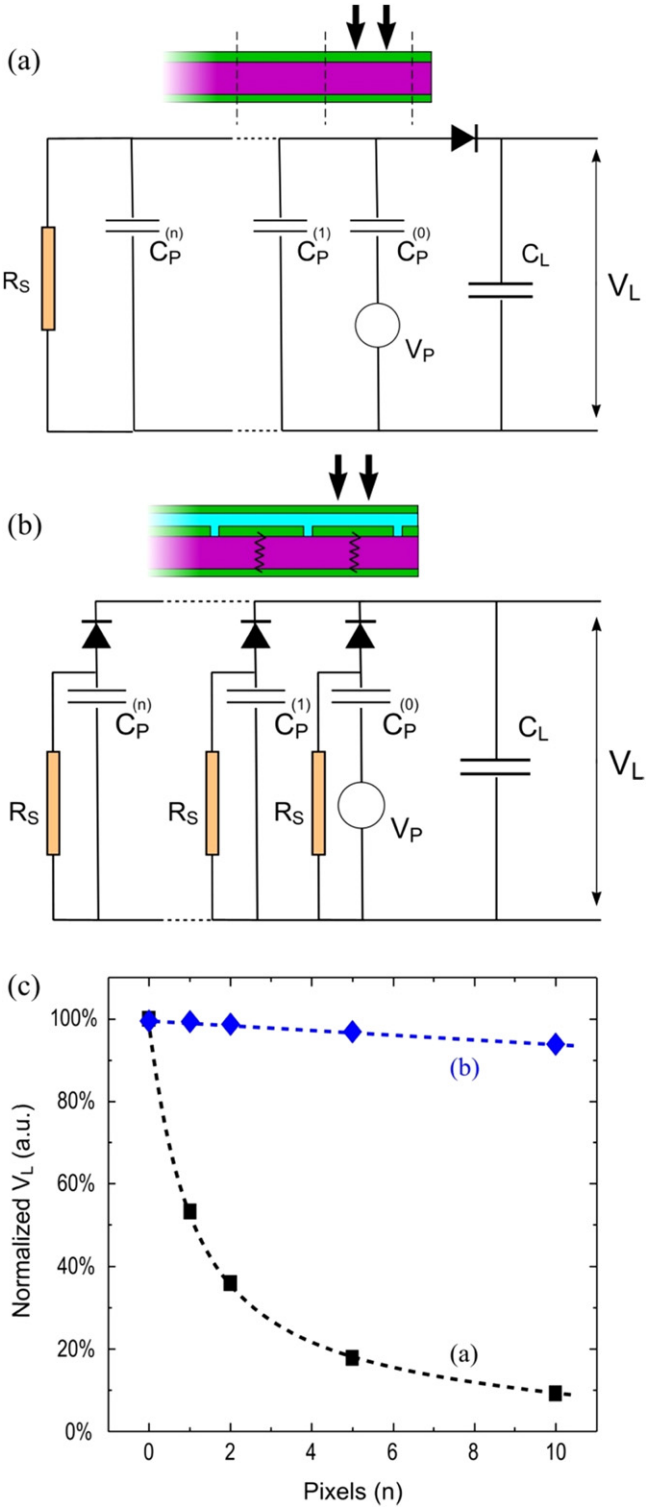

Figure 6. (a) Circuit model for a piezoelectric element under localized pressure. The rectifying diode and the capacitor C_L are added as external components. (b) Circuit model for a pixelated piezo-generator under localized pressure. Local R_S resistors and rectifying diodes are integrated into the structure for each pixel, and only the capacitor C_L is added as an external component. (c) Electrical simulation comparing the open circuit voltage V_L after 200 V_P pulses for the idealized circuits in (a) and (b), as a function of n.

[3] The rectifier was modeled as a diode with forward resistance of 1 k Ω, reverse resistance of 10 G Ω, and a threshold voltage of 10 mV. The voltage generated across a single piezoelectric pixel upon multiple pressure events was modeled as a train of 200 1V pulses with period of 500 ms and rise, on and fall times all set to 50 ms. The load capacitor was set to 1 μF.

circuit voltage V_L as a function of n, normalized to that obtained in the case of a single device or pixel ($n=0$). The simulation confirms that, for the circuit modeled in figure 6(a), the output voltage V_L decays rapidly with the number of pixels. Conversely, for the circuit in figure 6(b), the output shows only a very weak dependence on the number of pixels.

The message conveyed by figure 6 is of general validity. Even if the simulation is not tailored to our particular components (in fact, a conventional diode is not a good approximation for our QTC™ 'rectifier'), it sets down the requirements for the optimal architecture. For our device specifically, it is crucial to maximize the voltage output of a single pixel. Replacing a conventional diode with a pressure switch means that, if the stimulus voltage is not larger than the voltage already built into C_L, not only charge pumping does not occur, but some current can actually flow back from C_L towards the piezo-elements. The small drawing associated to figure 6(b) shows our proposed approach to turn a single integrated piezo-generator into a pixelated structure that mimics the optimal circuit geometry. One has only to pattern the metallic electrode on top of the piezoelectric material according to the expected stimulus area, and provide individual R_S connections to the bottom electrode. If the piezoelectric material itself has (or is engineered to have) an internal resistance within the suitable R_S tolerance (fairly wide, see supporting information), the implementation is straightforward. Note that there is no need to pattern the piezoresistive material, as this becomes locally conductive only where pressure is applied. For energy-harvesting applications, where the collective output of all pixels is funneled into a single capacitor (or battery) as in figure 6(b), there is no need to pattern the uppermost metal electrode either (because still $C_{QTC} \ll C_P$). On the other hand, if the pressure stimulus needs to be spatially resolved (e.g., for touchscreen applications), the uppermost metal electrode needs to be patterned into pixels that mirror those of the metallic electrode below. Such pixels must then be wired out independently by means of, e.g., a crossbar architecture.

It is worth comparing our technology and related implementations to the DC piezo-generator proposed by Wang's group [8] and further exploited in [4, 5]. Their approach based on vertically-aligned ZnO nanowires is ingenious: according to our understanding, each individual ZnO nanowire provides a piezoelectric drive via mechanical bending, a resistor R_S through itself (n-type ZnO is a poor conductor but not an insulator), and the equivalent of a rectifying diode via a mechanical ohmic/Schottky-contact switch at its tip. It is thus an alternative and feasible implementation of the optimal circuit geometry shown in figure 6(b). However, by the authors' own admission, there were problems with the output stability, mechanical robustness, lifetime and environmental adaptability of such devices, which eventually pushed them towards planar nanowire geometries [17, 18], or vertically-aligned nanowire arrays supported by a soft polymer matrix [18, 19]. However, as nanowires are clamped at both sides with either an ohmic or Schottky contact [17–19], the rectification mechanism exploited in [8] is lost. The PVDF-based piezo-electrochemical cell demonstrated in [9], on the other hand, preserves the rectification feature and seems to show better robustness, but it still faces the challenge of growing vertically-aligned TiO_2 nanotubes over large areas coupled with the need of sealing the $LiPF_6$ electrolyte in a solid and safe packaging. Moreover, it is mostly oriented to energy-harvesting and not truly optimized for sensing applications like touchscreens. Overall, our devices have an efficiency on par with [9], are very robust and durable, are much easier to fabricate, and are much more scalable toward very large areas, which makes them suitable for a wider range of applications.

Conclusions

As concluding remarks, we highlight a few additional points of practical interest. First, our technology is applicable to any piezoelectric material, hard or soft. For flexible and deformable devices, PVDF is ideal as it produces a larger output when allowed to bend under pressure [20]. Second, the whole integrated structure can in principle be made transparent, a compulsory feature for touchscreen applications. Indeed, transparent piezoelectric materials are common (quartz or PVDF), transparent electrodes can be made of ITO or graphene [21], and the piezoresistive QTC™ film is also available in a transparent form [11]. Transparent supercapacitors are also available, if needed [22, 23]. Finally, given the relatively thin-film nature of all layers involved, it is possible to stack many integrated piezo-generators together to maximize the energy harvested from a single stimulus. After taking all data and arguments into account, we believe that our integrated piezoelectric system possesses enough merits to suggest great potential as a viable commercial technology [24].

Acknowledgements

We thank G A J Amaratunga for useful discussion. We thank Measurement Specialties and Peratech for supplying us with the PVDF element and the QTC™ element, respectively.

References

[1] Rouvala M, Amaratunga G A J, Wei D and Colli A 2010 *Nanotechnologies for Future Mobile Devices* ed T Ryhanen, M A Uusitalo, O Ikkala and A Karkkainen (Cambridge, UK: Cambridge University Press) chapter 3
[2] Beeby S and White N 2010 *Energy Harvesting for Autonomous Systems* (Boston, MA: Artech House)
[3] Kim H S, Kim J-H and Kim J 2011 *Int. J. Precis. Eng. Man.* **12** 1129
[4] Choi M-Y, Choi D, Jin M-J, Kim I, Kim S-H, Choi J-Y, Lee S Y, Kim J M and Kim S-W 2009 *Adv. Mater.* **21** 2185
[5] Choi D *et al* 2010 *Adv. Mater.* **22** 2187
[6] Ramadass Y K and Chandrakasan A P 2010 *IEEE J. Solid-State Circuits* **45** 189

[7] Han J, von Jouanne A, Le T, Mayaram K and Fiez T S 2004 *19th Annu. IEEE Applied Power Electronics Conf. and Exposition* vol 3 p 1541
[8] Wang X, Song J, Liu J and Wang Z L 2007 *Science* **316** 102
[9] Xue X, Wang S, Guo W, Zhang Y and Wang Z L 2012 *Nano Lett.* **12** 5048
[10] McKay T G, O'Brien B M, Calius E P and Anderson I A 2011 *Appl. Phys. Lett.* **98** 142903
[11] Peratech Ltd 1998 UK *Patent* PCT/GB98/00206 (WO 98/33193)
[12] Bloor D, Donnelly K, Hands P J, Laughlin P and Lussey D 2005 *J. Phys. D: Appl. Phys.* **38** 2851
[13] Bloor D, Graham A, Williams E J, Laughlin P J and Lussey D 2006 *Appl. Phys. Lett.* **88** 102103
[14] Gamby J, Taberna P L, Simon P, Fauvarque J F and Chesneau M 2001 *J. Power Sources* **101** 109
[15] Stoller M D, Park S, Zhu Y, An J and Ruoff R S 2008 *Nano Lett.* **8** 3498
[16] Shirinov A V and Schomburg W K 2008 *Sensors Actuators* A **142** 48
[17] Yang R, Qin Y, Dai L and Wang Z L 2009 *Nat. Nanotechnol.* **4** 34
[18] Xu S, Qin Y, Xu C, Wei Y, Yang R and Wang Z L 2010 *Nat. Nanotechnol.* **5** 366
[19] Momeni K, Odegard G M and Yassara R S 2010 *J. Appl. Phys.* **108** 114303
[20] Mateu L and Moll F 2005 *J. Intell. Mater. Syst. Struct.* **16** 835
[21] Bonaccorso F, Sun Z, Hasan T and Ferrari A C 2010 *Nat. Photon.* **4** 611
[22] Chen P-C, Shen G, Sukcharoenchoke S and Zhou C 2009 *Appl. Phys. Lett.* **94** 043113
[23] Hiralal P, Wang H, Unalan H E, Liu Y, Rouvala M, Wei D, Andrew P and Amaratunga G A J 2011 *J. Mater. Chem.* **21** 17810
[24] Colli A and White R 2014 *Patent pending*